Citation: BoneKEy Reports **5**, Article number: 787 (2016) | doi:10.1038/bonekey.2016.14

www.nature.com/bonekey

ORIGINAL ARTICLE

Fam3c modulates osteogenic cell differentiation and affects bone volume and cortical bone mineral density

Jorma A Määttä[1,2,3], Ameya Bendre[1], Mervi Laanti[1], Kalman G Büki[1], Pia Rantakari[3,4], Päivi Tervola[1], Johanna Saarimäki[1], Matti Poutanen[3,4], Pirkko Härkönen[1] and Kalervo Väänänen[1]

[1]Department of Cell Biology and Anatomy, Institute of Biomedicine, University of Turku, Turku, Finland. [2]School of Pharmacy, University of Eastern Finland, Kuopio, Finland. [3]Turku Center of Disease Modeling, University of Turku, Turku, Finland. [4]Department of Physiology, Institute of Biomedicine, University of Turku, Turku, Finland.

Fam3c, a cytokine-like growth factor, has been suggested to have a role in epithelial-to-mesenchymal transition (EMT), tumor growth and metastasis. A single-nucleotide polymorphism affecting bone mineral density has been found in the first intron of the *Fam3c* gene in a study analyzing an Asian population cohort. Other independent studies on different population cohorts have found the *fam3c* locus to be associated with bone mineral density and fractures. In order to investigate the role of Fam3c in bone biology, we have generated a *Fam3c* knock-out (KO) mouse strain. The *Fam3c* KO mice were found to have normal appearance, behavior and fertility, but small changes in bone morphology and content were also observed. Micro-CT analysis of tibiae of the female mice revealed decreased number of trabeculae. In male mice the changes in the bone phenotype were smaller, but hematological changes were observed. Furthermore, there was a negative correlation between body weight and tibial trabecular and cortical bone volume in the male KO mice. There was a small increase in cortical bone mineral density, but in the lateral direction of tibiae the breaking strength was reduced. *Fam3c* KO bone marrow cells showed accelerated osteogenic differentiation and mineralization *in vitro*. The reduced number of bone trabeculae in *Fam3c* KO mice and the stimulated osteogenic differentiation indicate a role for Fam3c in osteoblast differentiation and bone homeostasis.

BoneKEy Reports **5**, Article number: 787 (2016) | doi:10.1038/bonekey.2016.14

Introduction

The family of sequence similarity 3c (Fam3c; also known as interleukin-like epithelial-to-mesenchymal transition (EMT) inducer—ILEI) is a cytokine-like growth factor which is widely expressed in adult tissues,[1,2] the function of which has been attributed to EMT, tumor growth and metastasis.[3,4] However, little is known about its function in addition to the role described in EMT. A large single-nucleotide polymorphism (SNP) analysis of a Korean population cohort revealed that a SNP affecting bone mineral density (BMD) at several skeletal sites is located at the first intron of the *Fam3c* gene.[5] A few later independent genome-wide studies, on different population cohorts, have also confirmed the association of Fam3c with BMD and fractures.[6–8] Recently, the structure of Fam3c was modeled[9] suggesting that Fam3c could interact via a distinct mechanism, as it possesses a non-cytokine-like fold. As of now, there is no published data regarding the receptor of Fam3c.

Bone homeostasis is regulated by a multitude of nutritional, biomechanical, hormonal and growth factors. Most of the bone is formed by endochondral ossification, wherein collagen matrix template is mineralized and subsequently remodeled. Bone is constantly resorbed and formed, leading to complete renewal of the skeleton ~4–5 times during human lifespan. The rate of bone formation and resorption is in balance during adulthood.[10]

Osteoblasts are bone cells responsible for new bone formation. Mesenchymal stromal cells (MSCs) in the bone marrow undergo differentiation into osteoprogenitor cells, which subsequently further differentiate into mature osteoblasts.[11] Many transcription factors, growth factors and signaling pathways have been shown to regulate osteoblast

Correspondence: Dr JA Määttä, Department of Cell Biology and Anatomy, Institute of Biomedicine, University of Turku, Kiinamyllynkatu 10, Turku FI20520, Finland. E-mail: jmaatta@utu.fi

Received 5 October 2015; accepted 22 January 2016; published online 6 April 2016

differentiation. These include factors such as Sox9,[12] Runx2, Osterix,[13,14] bone morphogenic proteins and SMADs,[15] Indian hedgehog,[12] Wnt/β-catenin[16] transforming growth factor-β (TGFβ), insulin-like growth factor-1, parathyroid hormone (PTH), PTH-related peptide and fibroblast growth factors.[17–20]

A major cytokine affecting bone metabolism is TGFβ which regulates osteoblast proliferation and migration and inhibits osteocyte apoptosis.[21] Furthermore, TGFβ has been recently shown to inhibit osteogenic differentiation of bone marrow-derived MSCs by downregulating the Wnt/β-catening signaling pathway by upregulating DKK1 and GSK-3β expression.[22] TGFβ has been suggested to be an upstream regulator of *Fam3c* as it activates *Fam3c* translation by inducing disengagement of translational silencers from the Fam3c mRNA.[3,23] The secretion of Fam3c and the conversion of the propeptide form of Fam3c to active protein are regulated by the plasminogen-urokinase-plasminogen receptor system. whereas in serum it is converted to its active form by serum proteases.[24]

Osteoporosis is a condition affecting largely postmenopausal women and also a significant proportion of elderly men. Osteoporosis leads to a significant reduction in the quality of life and increasing health-care costs because of fractures. To find effective treatment options, it is important to expand our knowledge about the regulation of bone tissue and the roles of different proteins involved. *Fam3c* gene has been shown to be an important determinant of BMD at the population level.[5] A mouse model where the *Fam3c* gene is inactivated has been previously generated.[25] Previously no significant bone phenotype could be consistently associated with the gene inactivation in mice.[25] In this communication, we for the first time show that genome-wide inactivation of the *Fam3c* gene in mice leads to alterations in the trabecular and cortical bone structure and volume, and cortical BMD (Ct.BMD). Taken together, these changes in bone structure cause a marked reduction in bone strength. Moreover, correlation of body weight (BW) to cortical and trabecular bone volume (BV) was altered in the knock-out (KO) mice. In addition, the *in vitro* differentiation of bone marrow-derived MSCs to osteoblasts was also accelerated in the KO mice suggesting a putative role of Fam3c in the regulation of osteoblast differentiation.

Results

General phenotype and blood analysis

The efficacy of *Fam3c* gene silencing was demonstrated by immunoblotting, showing strong protein expression of *Fam3c* in the spleens of WT mice and total lack of Fam3c protein in KO mice (**Figure 1b**).

Fam3c KO mice were apparently normal, fertile and their weight gain was similar to their wild-type (WT) counterparts (**Figure 1c and d**). Characteristic to mice with 129/C57BL/6N, 1:1 genetic background the fur color varied from black to almost white on both *Fam3c* WT and *Fam3c* KO mouse lines. No abnormalities were observed in a routine analysis of the histology of a large assortment of soft tissues: esophagus, stomach, jejunum, ileum, colon, rectum, pancreas, kidney, adrenal gland, trachea, lung, heart, cerebellum, cerebrum, pituitary gland, eye, salivary gland, thyroid gland, spleen, lymph node, thymus, skeletal muscle, testicles, epididymis, bladder, prostate, seminal vesicle, ovary and uterus (data not shown). Analysis of various blood cell types showed elevated numbers of polymorphonuclear neutrophils and reduced amounts of lymphocytes in male mice. The red blood cell counts were also higher (**Table 1**; 11.52 vs $9.77 \times 10^9\,ml^{-1}$, $P = 0.049$) but the mean corpuscular volume of the cells was slightly smaller in KO than in normal male mice (**Table 1**; 51.03 vs 52.73 fl, $P = 0.006$). The amount of mean corpuscular hemoglobin concentration was also smaller in male KO mice than in WT mice (**Table 1**; 14.98 vs 16.22 pg, $P < 0.001$). This is not, however, manifested as anemia because total hemoglobin did not differ significantly. No significant differences were found between blood cell

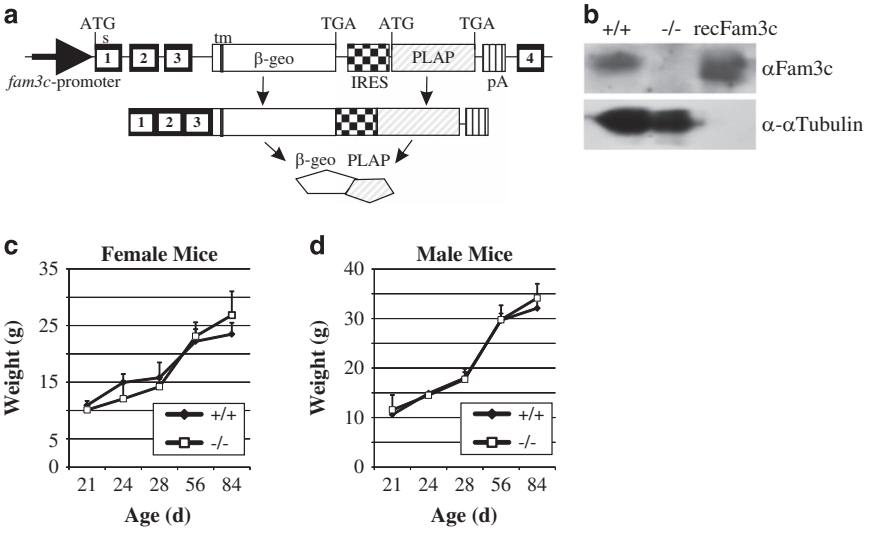

Figure 1 Generation of the *Fam3c* KO mouse. (**a**) Schematic illustration of the gene modification leading to inactivation of the *fam3c* gene and expression of the reporter construct. Gene-trap cassette was located within an intron between the exons 3 and 4 of the *fam3c* gene. This yields to expression of an mRNA encoding the first 3 exons on the *fam3c* gene, a sequence encoding β-galactosidase and neomycin resistance fusion protein (β-geo), intracistronic ribosome entry side and placental alkaline phosphatase. (**b**) Western blot of splenic lysate from *Fam3c* WT (+/+) and KO (−/−) mice. Recombinant Fam3c (50 ng) was used as a positive control. No Fam3c protein could be detected from −/− mice. The brightness and contrast were adjusted for optimal clarity. No significant differences were detected in the weight gain of WT and KO female (**c**) and male (**d**) mice.

counts or morphology between WT and KO female mice (**Table 1**).

Analysis of the reporter-gene expression in bone

To reveal the activity of the *Fam3c* promoter in bone of adult mice expression of the reporter β-galactosidase activity in KO mice was demonstrated in proliferating and hypertrophic chondrocytes of tibial growth-plate osteoclasts and osteoblasts (**Figure 2a**), periosteal cells (**Figure 2c**) and in some osteocytes of cortical bone (**Figure 2d**). Further to that, articular chondrocytes, especially at the lateral corners of the synovial surface, were strongly positive for the reporter-gene activity (**Figure 2f**) as well as the fibroblasts at the attachment of ligaments (**Figure 2h**). No staining was detected in the WT controls lacking the reporter construct (**Figure 2b, e and g**).

Analysis of the trabecular bone phenotype

Micro-CT analysis of 3-month-old female mice revealed that in *Fam3c* KO mice the tissue volume (TV) of tibial metaphysis was significantly increased compared with *Fam3c* WT counter pairs (2.6 vs 2.2 mm^3, $P = 0.002$; **Figure 3a**). This was accompanied by an increased trabecular separation (0.20 vs 0.30 mm, $P < 0.001$; **Figure 3a**) and decreased trabecular number (3.0 vs 2.5 mm^{-1}, $P = 0.049$; **Figure 3a**), but there was not a significant difference in BV (**Figure 3a**) all indicating that the same volume of bone is distributed to a larger TV in the female KO mice. In 7-month-old female mice, the trabecular number was even more reduced (0.25 vs 0.39 mm, $P < 0.001$; **Figure 3a**) leading to a significant reduction in the BV (0.30 vs 0.47 mm^3, $P = 0.003$; **Figure 3a**) and BV/TV ratio (9.8 vs 17.2% mm, $P < 0.001$; **Figure 3a**).

In 3-month-old male mice, the TV of tibial metaphysis was slightly elevated in KO mice as compared with WT mice (3.9 vs 3.7 mm^3, $P = 0.009$; **Figure 3a**), whereas in 7-month-old male mice the situation was the opposite (3.7 vs 4.5 mm^3, $P = 0.021$; **Figure 3a**). There was no significant difference in any other parameters of the tibial trabecular bone analyzed (**Figure 3a**).

Table 1 Blood composition analysis

	Female	*Average*	*± s.d.*	*Male*	*Average*	*± s.d.*
WBC ($\times 10^6$ ml^{-1})	WT	11.45	± 2.21	WT	10.25	± 1.65
	KO	9.58	± 1.65	KO	9.71	± 0.64
Neutrophils (%)	WT	7.15	± 1.58	WT	11.93	± 2.58**
	KO	12.16	± 4.16	KO	16.18	± 1.17
Lymphocytes (%)	WT	85.85	± 6.52	WT	82.05	± 3.71*
	KO	82.66	4.22	KO	77.28	± 1.66
Monocytes (%)	WT	0.98	± 0.34	WT	1.17	± 0.40
	KO	1.68	± 0.96	KO	2.03	± 0.67
Eosinophils (%)	WT	2.28	± 2.25	WT	2.38	± 0.87
	KO	1.28	± 0.40	KO	2.48	± 2.54
Basophils (%)	WT	0.40	± 0.08	WT	0.33	± 0.05
	KO	0.28	± 0.08	KO	0.33	± 0.13
RBC ($\times 10^9$ ml^{-1})	WT	9.82	± 0.39	WT	9.77	± 0.18*
	KO	10.34	± 0.26	KO	11.52	± 1.10
HGb ($mg\,ml^{-1}$)	WT	158.25	± 4.35	WT	158.33	± 3.14
	KO	160.20	± 1.79	KO	172.50	± 17.25
HCT (%)	WT	51.28	± 1.42	WT	51.55	± 1.54
	KO	53.44	± 1.46	KO	58.73	± 5.07
MCV (fl)	WT	52.03	± 1.80	WT	52.73	± 0.91**
	KO	51.62	± 2.19	KO	51.03	± 0.56
MCH (pg)	WT	16.13	± 0.68	WT	16.22	± 0.16***
	KO	15.50	± 0.55	KO	14.98	± 0.10
MCHC ($mg\,ml^{-1}$)	WT	310.00	± 3.56	WT	307.67	± 6.15*
	KO	300.60	± 7.77	KO	289.00	± 12.36
Platelets ($\times 10^6$ ml^{-1})	WT	943.5	± 249.2	WT	1051.00	± 66.5
	KO	1072.0	± 108.4	KO	1035.00	± 231.1

Abbreviations: HCT, ; HGb, hemoglobin; KO, knock out; MCH, mean corpuscular hemoglobin; MCHC, MCH concentration; MCV, mean corpuscular volume; RBC, red blood cell; WBC, white blood cell; WT, wild type. Blood samples ($n = 6$ per group) were analyzed with an Advia 120 instrument (Bayer-Siemens). The percentage of neutrophils out of WBCs was significantly increased and lymphocytes reduced in male KO mice as compared with male WT mice. Also red blood cell count was higher in male KO mice than in male WT mice. The MCH was also reduced in male KO mice, as well as MCV and MCHC.

Analysis of the cortical bone phenotype

In 3-month-old female mice, the BV/TV ratio of cortical bone was slightly decreased in KO mice when compared with WT mice (63.1 vs 66.4%, $P = 0.031$; **Figure 3b**). This was owing to increased TV (0.23 vs 0.21 mm^3, $P = 0.015$; **Figure 3b**), which was reflected as increased tissue area (T.Ar; 1.45 vs 1.30 mm^2, $P = 0.015$; **Figure 3b**) and endocortical area (Ec.Ar; 0.54 vs 0.43 mm^2, $P = 0.012$). There was no significant difference in cortical thickness and bone perimeter (B.Pm) although the medians of these parameters were slightly elevated in KO mice, which is consistent with the differences in TV, T.Ar and Ec.Ar (**Figure 3b**). In 7-month-old female mice, the TV was even more increased and BV/TV ratio reduced in the KO mice as compared with the WT mice (0.26 vs 0.22 mm^2, $P = 0.001$ and 63.8 vs 74.3%, $P < 0.001$, respectively; **Figure 3b**). This was accompanied by an increased B.Pm (10.5 vs 9.7 mm, $P = 0.045$), T.Ar (1.63 vs 1.35 mm^2, $P = 0.001$) and Ec.Ar (0.59 vs 0.35 mm^2, $P < 0.001$). Interestingly, the BMD was also elevated in the KO mice (1.10 vs 0.97 $g\,cm^{-3}$, $P = 0.012$). As shown in **Figure 3c**, in 3-month-old male mice the cortical BV/TV ratio was decreased in KO mice as compared with WT mice (57.0 vs 61.4%, $P < 0.001$) and Ec.Ar increased (0.81 vs 0.64 mm^2, $P = 0.011$). The Ct.BMD was higher in KO mice (1.08 vs 0.99 $g\,cm^{-3}$, $P = 0.035$). However, the difference in cortical BV/TV ratio was reversed in 7-month-old mice, where the BV/TV was slightly higher in KO mice when compared with WT (61.5 vs 57.3%, $P = 0.011$) mice and Ec.Ar correspondingly decreased (0.65 vs 0.78 mm^2, $P = 0.038$). The mean Ct.BMD was still higher in KO mice although the difference was not any more statistically significant (**Figure 3c**).

Break-point analysis

Three-point bending of tibial shafts at the distal attachment point of fibula revealed that in both sexes the break-point strength was significantly reduced in KO mice when compared with WT mice (**Table 2**, male mice, 19.8 N vs 25.3 N, $P < 0.001$; female mice 17.2 N vs 20.4 N, $P = 0.015$). In the male mice this was probably partly attributed to the altered bone geometry as the tibial shat was narrower at the site of analysis (**Table 2**). However, the thickness or the Ct.BMD of the tibial shafts of female KO and WT mice did not differ significantly (**Figure 3b**).

Correlation of BV to BW

In mammals BV has been shown to allotropically correlate with BW. The correlation trend between Tb.BV and BW was positive in 7-month-old WT mice, but significantly negative in KO mice (**Figure 4**). Also the correlation between Ct.BV and BW was clearly and significantly negative in male KO mice and positive in WT female mice (**Figure 4**). Moreover, the BW distribution was clearly wider in KO mice within this age group (**Figure 4**; 28–40 g

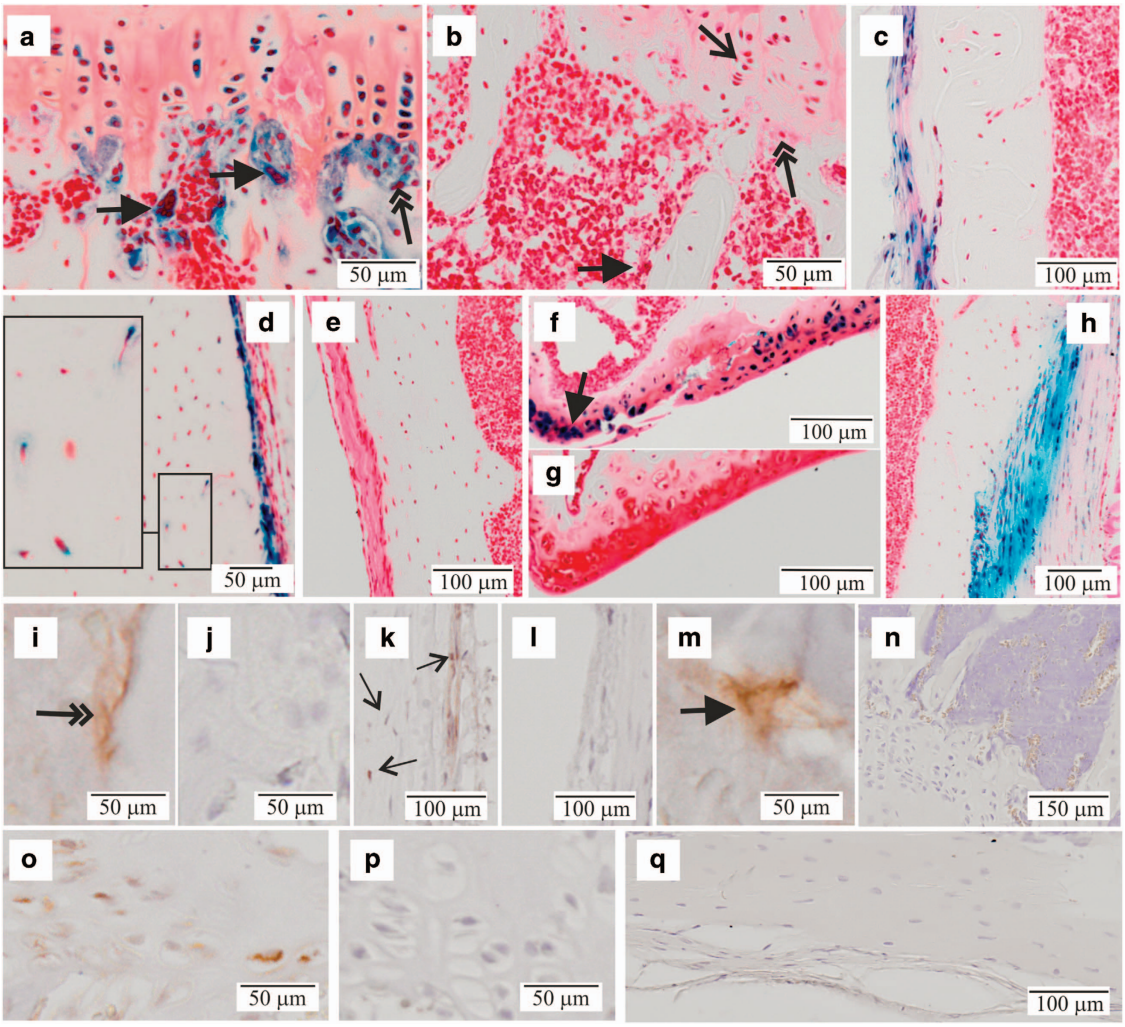

Figure 2 Reporter-gene activity in bone. Decalcified tibias from 8-week-old male and female mice were stained with x-gal for β-galactosidase activity and counter stained with safranin O. (**a**) Expression of the reporter gene was detected in osteoclasts (thick arrows), osteoblasts (double arrow) and proliferating growth-plate chondrocytes (thin arrow) as shown for (−/−) male mice. (**b**) Corresponding +/+ control for **a**. Periosteal cells were positive for the reporter (**c**) −/− male mouse and (**d**) −/− female mouse. Occasional positive osteocytes could be seen at the cortical bone of tibial diaphysis (**d**, inset). (**e**) +/+ control (female) from a similar location. (**f**) Chondrocytes of the articular cartilage were positive for the reporter showing most intense staining at the lateral edges of the knee joint (arrow, image form a −/− male mouse). (**g**) Corresponding +/+ control for **f**. (**h**) Attachment region of ligaments (shown for ligamentum collaterale mediale) were strongly positive for the reporter. The brightness and contrast were brought to visual uniformity between images. (**i–q**) Immunohistochemical staining with a polyclonal anti-Fam3c antibody. **i**, **k**, **m**, **o**, WT mice; **j**, **l**, **p** KO mice. (**n**, **q**) Conjugate controls with WT mice. (**i**,**j**) Immuno-positive osteoblasts indicated with a double arrow in **i**. (**k**, **l**) Periosteal cells and cortical bone osteocytes, immuno-positive cells indicated with arrows in **k**. (**m**) An immuno-positive osteoclast (thick arrow).

in WT vs 21–52 g in KO female mice and 41–47 g in WT vs 45–65 g in KO male mice). However, corresponding relationships between BW and BMD were not found (data not shown).

Bone histomorphometry

As shown in **Figure 5a**, the findings on trabecular bone obtained by conventional histomorphometry from a separate set of mouse samples were similar to those acquired with micro-CT (**Figure 3a and b**). In female mice the number of osteoclasts/T.Ar was decreased in KO mice when compared with WT mice (9.8 vs 17.2, $P = 0.046$). No significant differences were found in the number of osteoblasts (**Figure 5a**).

Osteogenic differentiation of bone marrow MSCs

Upon osteogenic differentiation the mRNA expression for tissue non-specific (bone) ALP was significantly higher at d9 and d15 in the osteogenic female KO bone marrow-derived MSC cell cultures than in WT cells (**Figure 5b**). The expression of collagen a1 mRNA was significantly stronger in KO cultures at d15 (**Figure 5c**) and also the osteocalcin mRNA, which was significantly stronger at d15 in KO culture than in the WT culture, where the osteocalcin mRNA began to emerge at d21 (**Figure 5d**). In male and female osteogenic MSC cultures, Von Kossa staining for the calcium precipitate/nodule detection displayed heavy staining earlier in male KO culture (d14) than in WT culture, where weak nodule formation was only detected at d21 (**Figure 5d**). In KO female culture the Von Kossa staining was similarly stronger, but later, at d21, only weak nodule formation was seen in the WT culture.

Discussion

In this communication we show for the first time that in addition to the suggested role in EMT, Fam3c is also involved in the

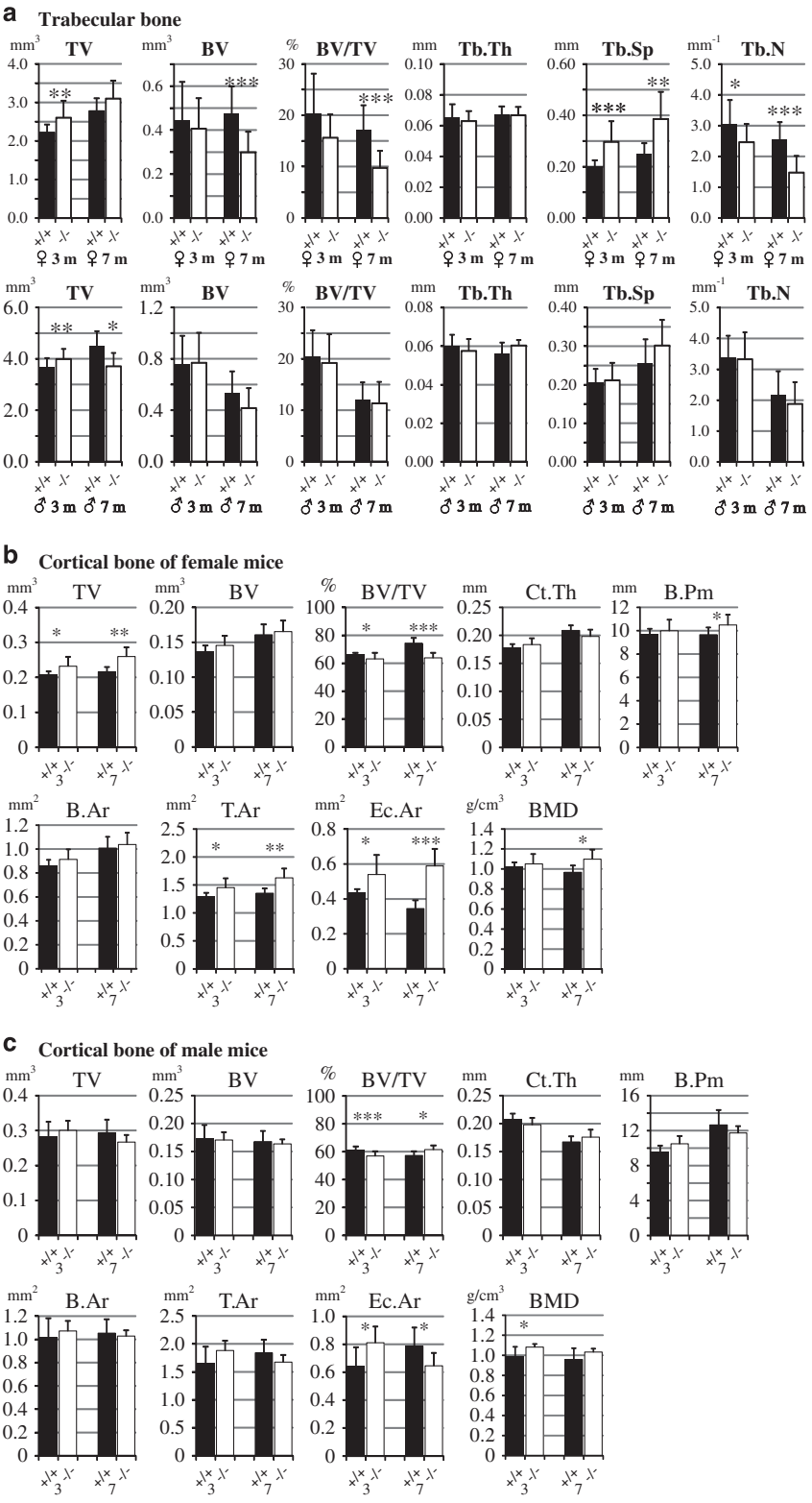

Figure 3 Micro-CT analysis of tibiae. (**a**) Trabecular bone of tibial metaphysis was analyzed from 3- and 7-month-old WT (+ / + , black bars) and KO (− / − , open bars) female and male mice. (**b**) Cortical bone of female mice and (**c**) male mice. For 3-month-old males: $n = 16$ WT, 21 KO mice; 3-month-old females: $n = 12$ WT, 21 KO mice; 7-month-old males: $n = 6$ WT, 11 KO mice; 7-month-old females; $n = 11$ WT, 8 KO mice. *$P < 0.05$; **$0.01 > P > 0.001$; ***$P < 0.001$.

regulation of MSC differentiation and BV. The reporter-gene activity for *Fam3c* expression was detected in all major bone cells and the expression was seen also with immunohistochemistry. Inactivation of the gene led to increased cortical mineral density. The latter observation might reflect in mice the *Fam3c*-allele-dependent cortical bone

density seen in human subjects[5–8] and was in line with the accelerated differentiation and mineralization seen in osteogenic cell culture of bone marrow cells.

Interestingly, the trabecular bone phenotype was clearly manifested in female mice, but not in males. This phenomenon was demonstrated by two independent methods (micro-CTand histomorphometry) used to analyze independent sets of samples. The gender difference in the manifestation of the bone phenotype might indicate that Fam3c could be involved in the sex hormone receptor-mediated signaling mechanisms in bone.[26,27] The reduction of Tb.BV is apparently contrary to the effects on BMD and osteogenic cell cultures. However, the formation of trabeculae is a sum of consorted actions of many bone cell populations, all of which are affected by the inactivation of Fam3c.

The allometric correlation of BW vs BV is well-established between various mammalian species.[28] The ability of the bone to adapt to mechanical load (mechanoreceptor-mediated signaling) is also a well-known phenomenon, the mechanisms of which are currently under intensive investigation.[29–31] Correlation of BMD and bone mineral content with human BW has been found in several studies.[32,33] Profound obesity has been shown to lead to diminished BMD and bone strength both in mice and men.[33,34] In many human studies, dual-energy x-ray absorptiometry analysis which does not take into account the bone geometry has been applied, thus introducing a possibility of a bias in the analysis.[35] In rodents, limited data exists about the physiological variation of BW vs BV. Nevertheless, we found that in *Fam3c* WT mice the trabecular BV increased upon increasing BW, whereas in *Fam3c* KO mice this correlation was disturbed. Furthermore, the regulation of BW appeared to be less strictly controlled in KO mice than in WT mice after the period of rapid growth of young animals. This was evident as the variation of BW was clearly wider in 7-month-old KO mice than in WT mice (see **Figure 4**). The breaking strength of the tibiae was reduced in both sexes despite the slightly higher Ct.BMD. This can be mostly attributed to the altered bone geometry (narrower tibiae in the lateral direction) especially in the males. The change in geometry may indicate change in the bone response to mechanical load. In females the difference in geometry was not so clear. This might indicate that there could be also alterations in the bone–collagen matrix. However, further studies would be needed to find out if the Fam3c hass a role in the bone mechanoreceptor function.

The observations on bone phenotype—and also BW—might be related to the major difference seen in the kinetics of *in vitro* osteogenic differentiation, wherein KO bone marrow cells displayed faster differentiation into mineralizing cells. However, there was no evidence of gross osteopetrosis, because in spite of slightly increased cortical BMD the amount of trabecular bone was reduced in KO mice. MSCs are a key component of the bone marrow niche, which also comprises many different cellular populations, for example, cells of the lymphoid and myeloid lineages, hematopoietic stem cells, endothelial cells, neuronal cells and osteoclasts.[36,37] Cells of the hematopoietic lineage are known to differentiate in the bone marrow niche and their differentiation is suggested to be regulated by different cellular populations residing in the niche.[38] The small changes in the number of neutrophils and lymphocytes and red blood cells manifested in the KO mice could result from an altered function of the osteoblasts.

Table 2 Break-point force, length and thickness of tibiae

	Length (mm)	*Thickness (mm)*	*Force (N)*
Male WT (8)	16.23 ± 0.64	1.66 ± 0.11	25.3 ± 2.5
Male KO (8)	15.86 ± 0.61	1.54 ± 0.06*	19.8 ± 2.5***
Female WT (8)	15.89 ± 0.52	1.41 ± 0.05	20.4 ± 1.9
Female KO (8)	15.82 ± 0.38	1.40 ± 0.11	17.2 ± 2.3*

Abbreviations: KO, knock out; WT, wild type. Tibiae from 3-month-old mice were used ($n = 8$ per group). The thickness was measured in the lateral direction at the proximal attachment of fibula. Breaking force was measured with a three-point bending device and the maximal force before breakage was recorded.

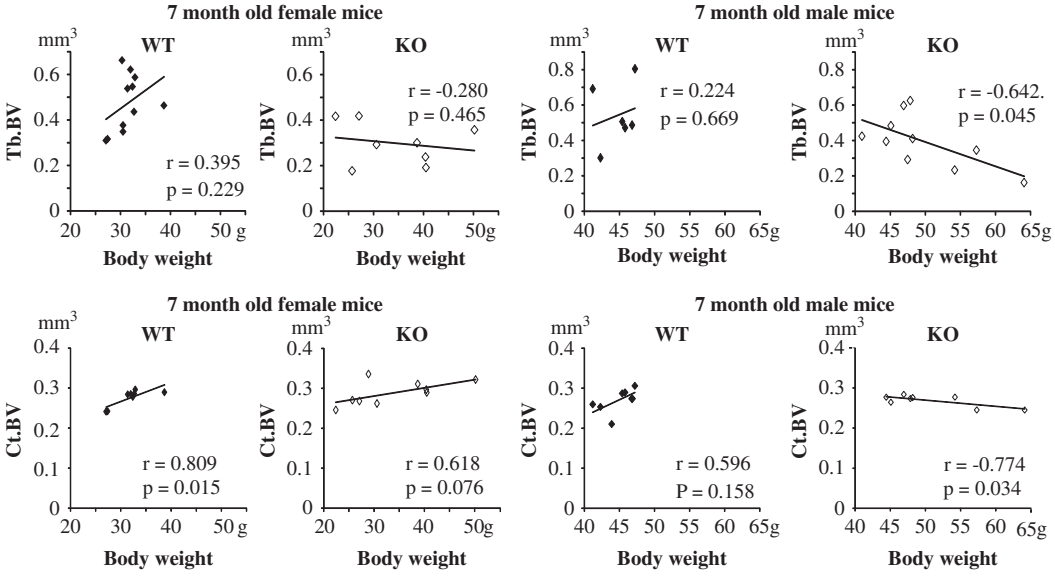

Figure 4 Correlation of BV to BW. In female WT mice, clear positive correlation was seen between Tb.BV and BW both in trabecular and cortical bone of tibiae form 7-month-old male and female mice. In male KO mice, the correlation between Tb.BV and BW and between Ct.BV and BW was negative. Also the variation of BW was wider in KO mice than in WT mice.

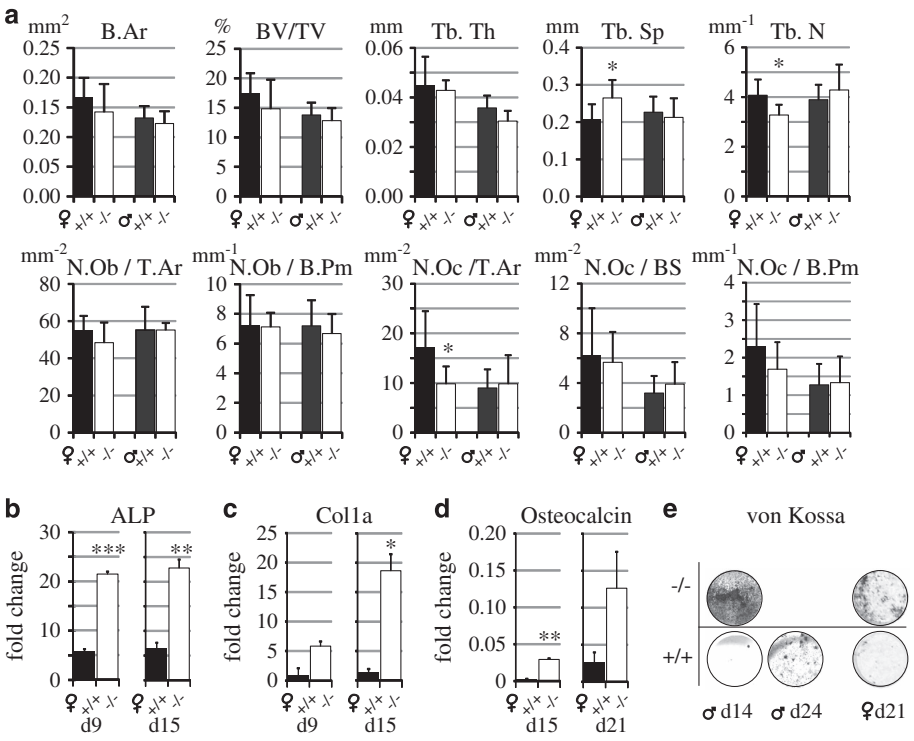

Figure 5 Histomorphometry of tibial metaphysis and osteogenic differentiation of bone marrow cells. (**a**) Histomorphometric analysis of tibial metaphysis of 3-month-old WT (+/+, black bars) and KO (−/−, open bars) female and male mice. The only significant difference was the reduced osteoclast number in female mice. $N = 8$ per group. RT-qPCR analysis of (**b**) ALP, (**c**) collagen 1a and (**c**) osteocalcin during osteogenic differentiation of bone marrow-derived MSCs of 8-week-old female WT and KO mice. (**e**) Von Kossa staining of a separate set of male and female KO and WT osteogenic cell cultures. KO cultures showed strong mineralization 1 week earlier that WT cultures. The brightness and contrast of the images were brought to visual uniformity. Similar results as shown in **b**, **c**, **d** and **e** were obtained from three independent experiments.

It is known that the Fam3c propeptide attaches to the extracellular matrix (ECM) through fibronectin.[24] On the other hand, fibronectin has been shown to regulate osteoblastic differentiation of human MSCs *in vitro*.[39] It could be hypothesized that the ECM-bound Fam3c could be released by resorbing osteoclasts and thus be involved in the signaling crosstalk between osteoclasts and osteoblasts.

Interestingly, expression of *Fam3c* has been shown to be regulated by upstream TGFβ signaling during the EMT in cancer cells.[3] Furthermore, this was confirmed in another study showing that TGFβ induces the translation of Fam3c mRNA by disengaging its translational silencer heterogeneous nuclear ribonucleoprotein E1.[23] TGFβ is present in the bone matrix and is released upon osteoclast-mediated resorption during bone remodeling.[40] It induces the migration of perivascular MSCs to the resorption site for osteoblast differentiation and new bone formation.[41] TGFβ signaling is mediated by the SMAD proteins and regulates the transcriptional activation of target genes.[42] TGFβ signaling also regulates mechanical properties and the mineral concentration of bone matrix.[43] *Fam3c* KO mice displayed accelerated osteogenic differentiation and mineralization. It could be hypothesized that TGFβ signaling induces the expression of *Fam3c* in bone cells and that Fam3c might be involved in the regulation of bone matrix properties and mineralization. The phenotype seen in *in vitro* osteogenic differentiation was, however, surprising. *In vivo* osteogenic differentiation is an intricately coordinated process. Many factors, for example, transcription activators, hormones, hematopoietic niche and crosstalk between different cellular populations, regulate the process. *In vitro* osteogenic differentiation takes place under much more simplified conditions, which would probably have allowed the effect of Fam3c during differentiation to be manifested.

Sex hormones and sex hormone receptor-mediated signaling mechanisms have been shown to regulate bone growth and composition.[26,27,44,45] The gender difference in the manifestation of the *fam3c*-related bone phenotype could be explained by the proposed mechanisms of how E2-mediated signaling is related to TGFβ production and the translational regulation of Fam3c mediated by TGFβ.[23,46,47]

One limitation of this study is that the gene inactivation was not cell specific. Therefore, it was not possible to deduce which bone cell population was mostly responsible for the bone phenotype observed. It is possible, that deletion of *Fam3c* could have disturbed its own regulatory system and therefore this could be responsible for a part of the phenotype observed. However, this is a universal concern regarding KO mouse models. However, based on our findings Fam3c is not a vital protein for mouse development. KO embryonic development was normal: the mice had normal outlook, fertility, behavior and lifespan. Instead, Fam3c appears to have a role in the fine tuning of bone morphology, BV and osteogenic differentiation.

Materials and Methods

Generation of *Fam3c* KO mice

The gene-trap clone LST057 was obtained from Bay Genomics (Mutant Mouse Regional Resource Centers, MMRRC, San

Francisco Bay Region, CA, USA). In that clone the gene-trap construct is integrated in the intron between exons 3 and 4 of the *Fam3c* gene in 129P2 (former 129/Ola) embryonic stem (ES) cells (**Figure 1a**). The 129P2 ES cells were injected into C57BL/N6 mouse blastocysts to generate chimeric mice. Breeding of the chimeras with C57BL/N6 mice produced heterozygous animals carrying the trapped allele. Heterozygous mice were used to generate mice homozygous for the WT and trapped (KO) *fam3c* allele. All the studies were carried out in mixed (129/C57BL/6N) genetic background. The C57BL/6N mice used as blastocyst donors were obtained from Charles River Laboratories (Wilmington, MA, USA). The mice were fed with a soya-free diet, and they were maintained in a specific pathogen-free stage at Central Animal Laboratory at the University of Turku, Turku, Finland. All studies carried out with the mice were approved by the Finnish Animal Ethics committee, complying with international guidelines on the care and use of laboratory animals. The corresponding licenses provided by the State Provincial Office and National Animal Experiment Board were: #2009-06915 and #2165/04.10.07/2015, respectively.

Blood analysis

Blood was collected in heparinized tubes by heart puncture, immediately after killing of 3-month-old mice. Complete blood analysis was performed with an Advia 120 Hematology System (Siemens Healthcare, Erlangen, Germany) at Clinical Research Services Turku (CRST, Turku, Finland).

Micro-CT computer tomography analysis

Micro-CT computer tomography was performed with Skyscan 1070 x-ray computer tomography scanner (Bruker, Madison, WI, USA) essentially as described previously.[44,45] Reconstruction of cross-sectional images was done with NRecon v1.4 software and data analysis and 3D model building by CTan 1.9.32 software, both from Skyscan (Bruker). Following parameters were applied for scanning $\times 55$ magnification (pixel resolution of 5.33 μm), x-ray tube voltage 72 kV, tube current 140 μA, x-ray filtration with a 0.25-mm aluminum filter. Exposure time was 3.9 s for each frame and the object was rotated in steps of 0.45° (total rotation angle = 182.45°). Parameters for transverse image reconstruction were as follows: dynamic range 0.0025–0.130 arbitrary units, smoothing level 3, beam hardening reduction 85%, ring artifact reduction level 7.

For analysis of trabecular bone, a volumetric region of interest was defined at the metaphysis of the tibia starting 20 layers (106.6 μm) below an anatomic marker, showing lower surface of the growth plate at the cross-sectional middle of the tibia, and extending 301 layers (1604 μm). Cortical bone was excluded from the region used for analysis of trabecular bone. For analysis of cortical bone a slice at the diaphysis of tibia starting 4100 μm below the growth plate and extending for 51 layers (272 μm) was defined.

Bone break-point analysis

Right femora of 3-month-old mice were extracted and stored in 40% ethanol until use. The length and lateral cross-sectional thickness of tibia were measured with a caliper. The breaking forces of tibiae were analyzed in lateral direction with a three-point bending device[48] at the distal attachment point of the fibula.

Cell culture

Osteogenic differentiation of bone marrow cells from 10-week-old mice was performed applying a protocol described by Morko *et al.*.[49] Bone marrow cells were isolated from the endosteal cavity of diaphysis of tibiae and femorae with aspiration with α-MEM supplemented with pre-screened 15% heat-inactivated FBS (Gibco, Thermo-Fischer Scientific, Waltham, MA, USA). Cells were further detached by extrusion with a syringe and 22-guage needle, pelleted and cultured in flasks at density 10^6 cells mm^{-2} in a-MEM supplemented with 15% heat-inactivated FBS, 10^{-8} M dexamethasone (Sigma-Aldrich, St.-Louis, MO, USA), 10 mM HEPES and penicillin/streptomycin (both from Gibco, Thermo-Fischer Scientific, Waltham, MA, USA). After 2 days of culture non-attached cells were removed and the medium replaced. After 1 week adherent cells forming colonies were detached with trypsin-EDTA (Gibco, Thermo-Fischer Scientific), washed, counted and plated on six-well plates (50 000 cells per well) or 24-well plates (20 000 cells per well). Osteogenic differentiation was started with medium containing 15% heat-inactivated FBS, 10 mM Na-β-glycerophosphate, 50 μg ml^{-1} ascorbate-2-phosphate and for the three initial days 10^{-8} M dexamethasone (all from Sigma-Aldrich).

Bone histology, immunohistochemistry and histomorphometry

Bone histology and histomorphometry were performed as previously described.[43,44] Briefly, left femorae was fixed with 10% phosphate-buffered formalin, decalcified with 14% EDTA for 2 weeks and embedded in paraffin. Tartrate-resistant acid cellular phosphatase was detected on deparaffinized sections (5-μm thick) with an Acid Phosphatase Leukocyte kit (Sigma-Aldrich). For immunohistochemistry antigen retrieval was done with standard microwave oven treatment in citrate buffer. An in-house made polyclonal rabbit anti-Fam3c antiserum (raised with recombinant rat Fam3c protein) was used at 1:500 dilution and immunoreaction was detected with a Vectastain ABC streptavidin-HRP, biotin goat-anti-rabbit system using 3,3′-diaminobenzidine as a chromogen (Vector Laboratories, Burlingame, CA, USA). The lengths of right tibiae were measured with a caliper. Subsequently they were fixed with 40% ethanol, embedded in methyl metacrylate, cut into 5-μm sections and stained with Masson-trichrome stain. Histomorphometry was done under light microscopy and with the aid of OsteomeasureXP 3.1.0.1 program and digital drawing equipment (Osteometrics, Decatur, GA, USA).

RNA extraction, cDNA synthesis and quantitative-PCR

RNA was extracted by using the Nucleospin RNA kit (Macherey-Nagel, Duren, Germany). Briefly, cells at different time points were lysed using the lysis buffer provided in the extraction kit. DNAse treatment and column-based purification was performed according to the kit instructions and RNA was eluted in RNAse-free water. cDNA synthesis was performed using the Dynamo cDNA kit (Thermo Fisher Scientific). Quantitative-PCR was performed on a CFX96 thermal-cycler (Biorad Labaratories, Hercules, CA, USA) with iTaq universal SYBR green (Biorad Labaratories). △△Ct method was used for relative quantification. β-Actin was used as a reference gene. D3 differentiation cDNA was used as a calibrator. Primers: tissue non-specific mouse alkaline phosphatase (liver/bone/kidney),

forward: 5′-GGGAGATGGTATGGGCGTCT-3′, reverse: 5′-AGG GCCACAAAGGGGAATTT-3′ (product size: 117 bp). Mouse osteocalcin: forward, 5′-CTGACAAAGCCTTCATGTCCAAG-3′, reverse: 5′-AGCAGGGTCAAGCTCACATA-3′ (product size: 131 bp). Mouse collagen a1: forward, 5′-CGATGGATTCCCG TTCGAGT-3′, reverse: 5′-GCTACGCTGTTCTTGCAGTG-3′ (product size: 132 bp). Each forward primer was designed to span an exon boundary to prevent amplification of genomic DNA.

Statistical analysis

The data are presented as means and standard deviations. Statistical significance was analyzed with two-tailed Student's test. Variance equality was analyzed with Levene's test. On the basis of the test, unequal variances were assumed between the groups. *P*-values of <0.05 were considered as statistically significant. All analyses were performed with IBM SPSS Statistics for Windows, version 21 (Armonk, NY, USA).

Conflict of Interest

KV is a member of the editorial board of the BoneKey Reports.

Acknowledgements

This work was supported by research grants from the Academy of Finland (#250917) and the Turku University Foundation (#9034). We thank Mrs Liudmila Shumskaya, Mrs Jessica Kähäri, Ms Soili Jussila, Mr Valtteri Rinne and Mr Jaakko Määttä for excellent technical aid.

References

1. Zhu Y, Xu G, Patel A, McLaughlin MM, Silverman C, Knecht K *et al.* Cloning, expression and initial characterization of a novel cytokine-like gene family. *Genomics* 2002; **80**: 144–150.
2. Pilipenko VV, Reece A, Choo DI, Greinwald Jr. JH . Genomic organization and expression analysis of the murine Fam3c gene. *Gene* 2004; **23**: 159–168.
3. Waerner T, Alacakaptan M, Tamir I, Oberauer R, Gal A, Brabletz T *et al.* ILEI: a cytokine essential for EMT, tumor formation and late events in metastasis in epithelial cells. *Cancer Cell* 2006; **10**: 227–239.
4. Lahsnig C, Mikula M, Petz M, Zulehner G, Schneller D, van Zijl F *et al.* ILEI requires oncogenic Ras for the epithelial to mesenchymal transition of hepatocytes and liver carcinoma progression. *Oncogene* 2009; **28**: 638–650.
5. Cho YS, Go MJ, Kim YJ, Heo JY, Oh JH, Ban HJ *et al.* A large-scale genome-wide association study of Asian populations uncovers genetic factors influencing eight quantitative traits. *Nat Genet* 2009; **41**: 527–534.
6. Zhang LS, Hu HG, Liu YJ, Li J, Yu P, Zhang F *et al.* A follow-up association study of two genetic variants for bone mineral density variation in Caucasians. *Osteoporos Int* 2012; **23**: 1867–1875.
7. Zhang L, Choi HJ, Estrada K, Leo PJ, Li J, Pei YF *et al.* Multistage genome-wide association meta-analyses identified two new loci for bone mineral density. *Hum Mol Genet* 2014; **23**: 1923–1933.
8. Chesi A, Mitchell JA, Kalkwarf HJ, Bradfield JP, Lappe JM, McCormack SE *et al.* A trans-ethnic genome-wide association study identifies gender-specific loci influencing pediatric aBMD and BMC at the distal radius. *Hum Mol Genet* 2015; **24**: 5053–5059.
9. Johansson P, Bernström J, Gorman T, Öster L, Bäckström S, Schweikart F *et al.* FAM3B PANDER and FAM3C ILEI represent a distinct class of signaling molecules with a non-cytokine-like fold. *Structure* 2013; **21**: 306–313.
10. Boyce BF, Zuscik MJ, Xing L. Biology of bone and cartilage. In: Thakker R (ed.) *Genetics of Bone Biology and Skeletal Disease.* Elsevier Academic Press: London, UK, 2012, 35–51.
11. Heino TJ, Hentunen TA. Differentiation of osteoblasts and osteocytes from mesenchymal stem cells. *Curr Stem Cell Res Ther* 2008; **3**: 131–145.
12. St-Jacques B, Hammerschmidt M, McMahon AP. Indian hedgehog signalling regulates proliferation and differentiation of chondrocytes and is essential for bone formation. *Genes Dev* 1999; **13**: 2072–2086.
13. Komori T, Yagi H, Nomura S, Yamaguchi A, Sasaki K, Deguchi K *et al.* Targeted disruption of Cbfa1 results in a complete lack of bone formation owing to maturational arrest of osteoblasts. *Cell* 1997; **89**: 755–764.
14. Nakashima K, Zhou X, Kunkel G, Zhang Z, Deng JM, Behringer RR *et al.* The novel zinc finger-containing transcription factor osterix is required for osteoblast differentiation and bone formation. *Cell* 2002; **108**: 17–29.
15. Hughes FJ, Collyer J, Stanfield M, Goodman SA. The effects of bone morphogenetic protein -2, -4, and -6 on differentiation of rat osteoblast cells *in vitro*. *Endocrinology* 1995; **136**: 2671–2677.
16. Gaur T, Lengner CJ, Hovhannisyan H, Bhat RA, Bodine PV, Komm BS *et al.* Canonical WNT signalling promotes osteogenesis by directly stimulating Runx2 gene expression. *J Biol Chem* 2005; **280**: 33132–33140.
17. Ornitz DM, Marie PJ. FGF signaling pathways in endochondral and intramembranous bone development and human genetic disease. *Genes Dev* 2002; **16**: 1446–1465.
18. Ornitz DM. FGF signaling in the developing endochondral skeleton. *Cytokine Growth Factor Rev* 2005; **16**: 205–213.
19. Jackson RA, Nurcombe V, Cool SM. Coordinated fibroblast growth factor and heparan sulphate regulation of osteogenesis. *Gene* 2006; **379**: 79–91.
20. Teplyuk NM, Haupt LM, Dombrowski C, Mun FK, Nathan SS, Lian JB *et al.* The osteogenic transcription factor Runx2 regulates components of the fibroblast growth factor/proteoglycan signaling axis in osteoblasts. *J Cell Biochem* 2009; **107**: 144–154.
21. Tang SY, Alliston T. Regulation of postnatal bone homeostasis by TGFβ. *BoneKey Rep* 2013; **2**: 255.
22. Guerrero F, Herencia C, Almadén Y, Martinez-Moreno JM, Montes de Oca A, Rodriguez-Ortiz ME *et al.* TGF-β prevents phosphate-induced osteogenesis through inhibition of BMP and Wnt/b-catenin pathways. *PLoS ONE* 2014; **9**: e89179.
23. Chaudhury A, Hussey GS, Ray PS, Jin G, Fox PL, Howe PH. TGFβ-mediated phosphorylation of hnRNP E1 Induces EMT via transcript-selective translational induction of Dab2 and ILEI. *Nat Cell Biol* 2010; **12**: 286–293.
24. Csiszar A, Kutay B, Schmidt U, Macho-Maschler S, Schreiber M, Alacakaptan M *et al.* Interleukin-like epithelia-to-mesenchymal transition inducer activity is controlled by proteolytic processing and plasminogen-urokinase plasminogen activator receptor system-regulated secretion during breast cancer progression. *Breast Cancer Res* 2014; **16**: 433.
25. Zheng HF, Tobias JH, Duncan E, Evans DM, Eriksson J. Paternoster L *et al.* WNT16 influences bone mineral density, cortical bone thickness, bone strength, and osteoporotic fracture risk. *PLoS Genet* 2012; **8**: e1002745.
26. Syed F, Khosla S. Mechanisms of sex steroid effects on bone. *Biochem Biophys Res Commun* 2005; **328**: 688–696.
27. Compston JE. Sex steroids and bone. *Physiol Rev* 2001; **81**: 419–447.
28. Barak MM, Liebermann DE, Hublin JJ. Of mice, rats and men: trabecular bone architecture in mammals scales to body mass with negative allometry. *J Struct Biol* 2013; **183**: 123–131.
29. Ehrlich PJ, Lanyon LE. Mechanical strain and bone cell function: a review. *Osteoporos Int* 2002; **13**: 688–700.
30. Robinson JA, Chatterjee-Kishore M, Yaworsky PJ, Cullen DM, Zhao W, Li C *et al.* Wnt/β-catenin signaling is a normal physiological response to mechanical loading in bone. *J Biol Chem* 2006; **281**: 31720–31278.
31. Sugiyama T, Price JS, Lanyon LE. Functional adaptation to mechanical loading in both cortical and cancellous bone is controlled locally and is confined to the loaded bones. *Bone* 2010; **46**: 314–321.
32. Ito M, Hayashi K, Uetani M, Yamada M, Ohki M, Nakamura T. Association between anthropometric measures and spinal bone mineral density. *Invest Radiol* 1994; **29**: 812–816.
33. Greco EA, Francomano D, Fornari R, Marocco C, Lubrano C, Papa V *et al.* Negative association between trunk fat, insulin resistance and skeleton in obese women. *World J Diabetes* 2013; **4**: 31–39.
34. Cao JJ, Sun L, Gao H. Diet-induced obesity alters bone remodeling leading to decreased femoral trabecular bone mass in mice. *Ann N Y Acad Sci* 2010; **1192**: 292–297.
35. Lochmüller EM, Miller P, Bürklein D, Wehr U, Rambeck W, Eckstein F. *In situ* femoral dual-energy X-ray absorptiometry related to ash weight, bone size and density, and its relationship with mechanical failure loads of the proximal femur. *Osteoporos Int* 2000; **11**: 361–367.
36. Mendez-Ferrer S, Michurina TV, Ferraro RF, Mazloom AR, Macarthur BD, Lira SA *et al.* Mesenchymal and haematopoietic stem cells form a unique bone marrow niche. *Nature* 2010; **466**: 829–834.
37. Ehninger A, Trumpp A. The bone marrow stem-cell niche grows up: mesenchymal stem cells and macrophages move. *J Exp Med* 2011; **208**: 421–428.
38. Anthony BA, Link DC. Regulation of hematopoietic stem cells by bone marrow stromal cells. *Trends Immunol* 2014; **35**: 32–37.
39. Mathews S, Bhonde R, Gupta PK, Totey S. Extracellular matrix protein mediated regulation of the osteoblast differentiation of bone marrow derived human mesenchymal stem cells. *Differentiation* 2012; **84**: 185–192.
40. Dallas SL, Rosser JL, Mundy GR, Bonewald LF. Proteolysis of latent transforming growth factor beta (TGF-beta) - binding protein 1 by osteoclasts. A cellular mechanism for release of TGF-beta from bone matrix. *J Biol Chem* 2002; **277**: 21352–21360.
41. Tang Y, Wu X, Lei W, Pang L, Wang C, Shi Z *et al.* TGF-beta1-induced migration of bone mesenchymal stem cells couples bone resorption with formation. *Nat Med* 2009; **15**: 757–765.
42. Crane JL, Cao X. Bone marrow mesenchymal stem cells and TGF-β signaling in bone remodeling. *J Clin Invest* 2014; **124**: 466–472.
43. Balooch G, Balooch M, Nalla RK, Schilling S, Filvaroff EH, Marshall GW *et al.* TGF-beta regulates the mechanical properties and composition of bone matrix. *Proc Natl Acad Sci USA* 2005; **102**: 18813–18818.
44. Määttä JA, Büki KG, Gu G, Alanne MH, Vääräniemi J, Liljenbäck H *et al.* Inactivation of estrogen receptor alpha in bone forming cells induces bone loss in female mice. *FASEB J* 2013; **27**: 478–488.
45. Määttä JA, Büki KG, Ivaska KK, Nieminen-Pihala V, Elo TD, Kähkönen T *et al.* Inactivation of the androgen receptor in bone forming cells leads to trabecular bone loss in adult female mice. *BoneKEy Rep* 2013; **2**: 440.

46. Miranda-Carboni GA, Guemes M, Bailey S, Anaya E, Corselli M, Peault B *et al.* GATA4 regulates estrogen receptor-alpha-mediated osteoblast transcription. *Mol Endocrinol* 2011; **25**: 1126–1136.
47. Güemes M, Garcia AJ, Rigueur D, Runke S, Wang W, Zhao G *et al.* GATA4 is essential for bone mineralization via ERα and TGFβ/BMP pathways. *J Bone Miner Res* 2014; **29**: 2676–2687.
48. Peng Z, Tuukkanen J, Zhang H, Jämsä T, Väänänen HK. The mechanical strength of bone in different rat models of experimental osteoporosis. *Bone* 1994; **15**: 523–532.
49. Morko J, Kiviranta R, Mulari MT, Ivaska KK, Väänänen HK, Vuorio E *et al.* Overexpression of cathepsin K accelerates the resorption cycle and osteoblast differentiation *in vitro*. *Bone* 2009; **44**: 717–728.